



MAX-PLANCK-GESELLSCHAFT

Martin W. Hess

Peter Benner

**Fast Evaluation of Time-Harmonic  
Maxwell's Equations Using the  
Reduced Basis Method**



MAX-PLANCK-INSTITUT  
FÜR DYNAMIK KOMPLEXER  
TECHNISCHER SYSTEME  
MAGDEBURG

**Max Planck Institute Magdeburg  
Preprints**

MPIMD/12-17

October 8, 2012

**Impressum:**

**Max Planck Institute for Dynamics of Complex Technical Systems, Magdeburg**

**Publisher:**

Max Planck Institute for Dynamics of Complex  
Technical Systems

**Address:**

Max Planck Institute for Dynamics of  
Complex Technical Systems  
Sandtorstr. 1  
39106 Magdeburg

[www.mpi-magdeburg.mpg.de/preprints](http://www.mpi-magdeburg.mpg.de/preprints)

# Fast Evaluation of Time-Harmonic Maxwell's Equations Using the Reduced Basis Method

Martin W. Hess\* and Peter Benner\*

## Abstract

The reduced basis method (RBM) generates low order models for the solution of parametrized partial differential equations (PDEs) to allow for efficient evaluation in many-query and real-time contexts.

We show the theoretical framework in which the RBM is applied to Maxwell's equations and present numerical results for model reduction in frequency domain. Using rigorous error estimators, the RBM achieves low order models under variation of material parameters and geometry.

The RBM reduces model order by a factor of 50 to 100 and reduces compute time by a factor of 200 and more for numerical experiments using standard circuit elements.

## Index Terms

Electromagnetic analysis, Maxwell equations, Reduced basis method (RBM), Reduced order systems.

## I. INTRODUCTION

**M**ODEL Order Reduction (MOR) for Maxwell's Equations arising from microwave semiconductor devices allows the evaluation of the transfer behaviour over any frequency range for large-scale models. In the parametric setting (PMOR), the transfer behaviour can be analysed under the additional variation of geometric or material parameters.

The electromagnetic components we consider are excited by ports, i.e. parts of the structure where external sources such as voltages and currents are applied. The transfer function is then given as the ratio between output and input signals (cf. [1], [2]).

There exist various algorithms for model reduction which have been applied to computational electromagnetics. For instance, the technique of modal expansion has been investigated in [3], the moment matching technique, also called asymptotic waveform evaluation, in [4] and [5], Padé via Lanczos model reduction in [6] and [7], Krylov subspaces [8], [9] or a two-step Lanczos scheme in [10]. A recent overview can be found in [2]. Besides in the transfer behaviour, model reduction techniques are also applied in maxwell eigenvalue problems [11]. Here, we will consider the reduced basis method (RBM) [12] which has become a very popular approach for reducing models described by partial differential equations (PDEs) in recent years. A first introduction of the RBM to microwave devices has been established in [13]. We extend the work of [13] to parametric models including geometric and material parameters besides frequency and apply rigorous error estimators including the estimation of the stability constant.

The strength of the reduced basis method is the capability to deal with parameter spaces  $D \subset \mathbb{R}^p$  of higher dimensions (like  $p > 3$ ) including frequency, geometric and material parameters all at once. Using rigorous error estimators for the construction of the reduced order model, a given approximation tolerance can be certified.

The starting point of the RBM [12] is the variational or weak form of a PDE, e.g.

$$a^e(u^e, v^e; \nu) = f^e(v^e; \nu), \quad \forall v^e \in X^e,$$

with field solution  $u^e$ , testfunctions  $v^e$  and parameter  $\nu \in D$ . The superscript  $e$  denotes the "exact", infinite dimensional formulation. After discretisation and Galerkin projection, the problem is turned into a discrete formulation of typically large dimension  $\mathcal{N}$

$$a(u, v; \nu) = f(v; \nu), \quad \forall v \in X.$$

Using solution snapshots at certain parameter values  $\nu$  to span a low order space  $X_N$ , one can perform another Galerkin projection onto the space of snapshots as

$$a(u_N, v_N; \nu) = f(v_N; \nu), \quad \forall v_N \in X_N \subset X.$$

For a well-chosen reduced basis space  $X_N$ , the low order solution approximates the full order solution in the sense of a small error  $\|u - u_N\|_X$ .

\*Max Planck Institute for Dynamics of Complex Technical Systems, Sandtorstr. 1, 39106 Magdeburg, Germany (hessm@mpi-magdeburg.mpg.de, benner@mpi-magdeburg.mpg.de).

The RBM shows up to exponential convergence rates and generates low order models usually,  $N < 100$ . The approximation quality is satisfied with the use of rigorous error estimators.

Section 2 outlines the constitutive equations under consideration and gives basic definitions and terminology from functional analysis required for reduced basis model reduction. Section 3 describes the reduced basis model reduction algorithm, including details for efficient implementation, while the most technical part of the error estimation can be found in Appendix A. Section 4 shows the performance of the RBM on two example models and contains numerical results, while Section 5 gives concluding remarks and related further research topics.

## II. PROBLEM STATEMENT

Investigating the transfer behavior of microwave semiconductor devices requires the solution of the system equations for many frequencies and geometric parameters. This quickly exceeds available computational time when performed on the full order model. Using the examples of a coplanar waveguide and a branchline coupler, we investigate the performance of the RBM. The central idea of the RBM is to project the system equations onto a space of low order, which properly approximates the parametric manifold of the state space in the desired parameter range.

### A. Full time-harmonic Maxwell's equations

We consider the second order time-harmonic formulation of Maxwell's equations for the electric field  $E$

$$\nabla \times \mu^{-1} \nabla \times E + j\omega\sigma E - \omega^2 \epsilon E = j\omega J, \quad (1)$$

in  $\Omega \subset \mathbb{R}^d$  ( $d = 2, 3$ ) with source term  $J$ , permeability  $\mu$ , conductivity  $\sigma$ , permittivity  $\epsilon$  and subject to zero electric (PEC) and magnetic (PMC) boundary conditions

$$E \times n = 0 \quad \text{on } \Gamma_{\text{PEC}}, \quad (2)$$

$$\nabla \times E \times n = 0 \quad \text{on } \Gamma_{\text{PMC}}, \quad (3)$$

such that  $\partial\Omega = \Gamma_{\text{PEC}} \cup \Gamma_{\text{PMC}}$ .

By multiplying (1) with a test function  $v$ , we arrive at the variational or weak formulation

$$\begin{aligned} (\mu^{-1} \nabla \times E, \nabla \times v) + j\omega(\sigma E, v) - \omega^2(\epsilon E, v) \\ = j\omega(J, v), \end{aligned} \quad (4)$$

where  $(\cdot, \cdot)$  denotes the complex  $L^2$  inner product over the computational domain  $\Omega$ . The relevant function space over which the weak form is posed is  $H(\text{curl})$ , defined as

$$H(\text{curl}) := \{v \in [L^2(\Omega)]^3 \mid \nabla \times v \in [L^2(\Omega)]^3\}. \quad (5)$$

After discretization with  $H(\text{curl})$ -conforming Nédélec finite elements (cf. [14], [15]), solving (4) reduces to solving a sparse linear system

$$Ax = b, \quad (6)$$

for the state vector  $x \in \mathbb{C}^{\mathcal{N}}$  of large dimension  $\mathcal{N}$ , which represents the electric field solution  $E$ . The discrete space  $X$  is composed of basis functions  $\{\phi_j \mid j = 1, \dots, \mathcal{N}\}$ , s.t.

$$X = \text{span}\{\phi_j \mid j = 1, \dots, \mathcal{N}\}. \quad (7)$$

When we are only interested in the transfer behaviour over a certain frequency range (i.e.  $\nu = \omega$ ), the matrix  $A$  can be seen as an affine composition of parameter-independent matrices  $A^\mu$ ,  $A^\sigma$  and  $A^\epsilon$ , as

$$A = A^\mu + j\omega A^\sigma - \omega^2 A^\epsilon, \quad (8)$$

where the matrices are defined element-wise by

$$A_{ij}^\mu = (\mu^{-1} \nabla \times \phi_i, \nabla \times \phi_j), \quad (9)$$

$$A_{ij}^\sigma = (\sigma \phi_i, \phi_j), \quad (10)$$

$$A_{ij}^\epsilon = (\epsilon \phi_i, \phi_j). \quad (11)$$

PEC boundary conditions are incorporated by setting the appropriate degrees of freedom to zero and PMC boundary conditions are treated as natural boundaries.

Splitting the state vector  $x$  into real and complex parts  $x = x_{real} + jx_{imag}$  and using (8), the complex linear system can be rewritten as an equivalent system of twice the dimension over the real numbers

$$\begin{bmatrix} A^\mu - \omega^2 A^\epsilon & -\omega A^\sigma \\ -\omega A^\sigma & -A^\mu + \omega^2 A^\epsilon \end{bmatrix} \begin{bmatrix} x_{real} \\ x_{imag} \end{bmatrix} = \begin{bmatrix} 0 \\ -b \end{bmatrix}. \quad (12)$$

This leads to a real and symmetric system matrix, thus its spectrum is real, which is advantageous for the computation of eigenvalues required in the error estimation process.

Let  $u$  denote the solution vector of (12) and consider the real bilinear form  $a(\cdot, \cdot; \nu)$  defined over the  $H(\text{curl})$  conforming finite element space  $X$  by the system matrix  $A^\nu$  from (12) as

$$\begin{aligned} a(u, v; \nu) &= u^T A^\nu v \\ &= u^T \begin{bmatrix} A^\mu - \omega^2 A^\epsilon & -\omega A^\sigma \\ -\omega A^\sigma & -A^\mu + \omega^2 A^\epsilon \end{bmatrix} v. \end{aligned} \quad (13)$$

### B. Affine Decomposition

The efficient use of the RBM requires an affine decomposition, i.e. a decomposition of the parameter-dependent bilinear form  $a(\cdot, \cdot; \nu)$  into parameter-independent bilinear forms  $a^q(\cdot, \cdot)$  and parameter-dependent coefficient functions  $\Theta_a^q(\nu)$ , as

$$a(u, v; \nu) = \sum_{q=1}^{Q_a} \Theta_a^q(\nu) a^q(u, v). \quad (14)$$

In the case of only having the frequency  $\omega$  as parameter, the affine form is readily established, by expanding (12) in the frequency. Material parameters also readily allow an affine expansion, as the weak form (4) already is affine in  $\mu, \sigma$  and  $\epsilon$ . An affine decomposition (14) enables fast (i.e.  $\mathcal{N}$ -independent) evaluations of the input-output behaviour of the reduced model as well as the error estimator. In case of a nonaffine parameter dependence, an affine form can be approximated by using the empirical interpolation method [16].

### C. Geometric Parameters

In case of a geometric parameter dependency the computational domain is written as  $\Omega = \Omega(\nu)$ . As a remeshing of the computational domain for each parameter configuration is not feasible, an affine transformation to a reference configuration  $\Omega(\bar{\nu})$  is used.

First the computational domain  $\Omega(\nu)$  is partitioned into disjoint regions  $\Omega^k(\nu)$ , such that there exist affine mappings  $T^k$  from the respective regions of the reference configuration to the real configuration

$$\begin{aligned} T^k : \Omega^k(\bar{\nu}) &\rightarrow \Omega^k(\nu) : \\ x &\mapsto y = G(\nu)x + D(\nu), \quad \text{with} \\ G(\nu) &\in \mathbb{R}^{3 \times 3}, \quad D(\nu) \in \mathbb{R}^3. \end{aligned}$$

Many geometric variations allow such a decomposition: the example section shows a geometric variation in a coplanar waveguide. The affine mappings are piecewise bijective and collectively continuous, so that a global mapping  $T$  can be defined by

$$T : \Omega(\bar{\nu}) \rightarrow \Omega(\nu) : x \mapsto y = T^k(x) \quad \forall x \in \Omega^k(\bar{\nu}). \quad (15)$$

Thus, the PDE can be transformed [17] to the reference domain, using standard FE-transformations of  $H(\text{curl})$  with the Piola transformation

$$\begin{aligned} &\int_{T(\Omega(\bar{\nu}))} \mu^{-1} (\nabla \times E, \nabla \times v) + i\omega\sigma(E, v) - \omega^2\epsilon(E, v) dy \\ &= \int_{\Omega(\bar{\nu})} \mu^{-1} G^{-1}(\nu) (\nabla \times E, \nabla \times v) G^{-T}(\nu) |\det G(\nu)| \\ &\quad + G^T(\nu) (i\omega\sigma(E, v) - \omega^2\epsilon(E, v)) G(\nu) \frac{1}{|\det G(\nu)|} dx, \end{aligned} \quad (16)$$

which allows an affine decomposition (14) and also to rewrite the system into a real symmetric form (13).

#### D. Basic Definitions

The discrete variational form (13) is posed over the function space  $X = H(\text{curl})$ . We define the dual space  $X'$  as the space of linear functionals  $\phi : X \rightarrow \mathbb{R}$ . The dual norm is defined as

$$\|\phi\|_{X'} = \sup_{v \in X} \frac{|\phi(v)|}{\|v\|_X}. \quad (17)$$

According to the Riesz representation theorem, the spaces  $X$  and  $X'$  are isometrically isomorph, i.e. for each  $\phi \in X'$  there exists a unique  $v \in X$  such that  $\phi(\cdot) = (v, \cdot)_X$  and  $\|\phi\|_{X'} = \|v\|_X$ . In particular, it holds that  $f(\cdot; \nu) \in X'$  and  $a(u, \cdot; \nu) \in X'$ .

The inf-sup stability constant  $\beta(\nu)$  is defined as

$$\beta(\nu) = \inf_{u \in X} \sup_{v \in X} \frac{|a(u, v; \nu)|}{\|u\|_X \|v\|_X} \quad (18)$$

$$= \inf_{u \in X} \frac{\|a(u, \cdot; \nu)\|_{X'}}{\|u\|_X}. \quad (19)$$

The system (6) is uniquely solvable when  $\beta(\nu) > 0$ , in the case of  $\beta(\nu) = 0$  a resonance configuration is found. Lower bound estimates  $\beta_{LB}(\nu) \leq \beta(\nu)$  are constructed within a Successive Constraint Method (SCM) (see [18] and the Appendix), which are used for error estimation.

Further define the supremizing operator  $T^\nu : X \rightarrow X$  by

$$(T^\nu u, \cdot) = a(u, \cdot; \nu), \quad (20)$$

such that  $T^\nu u$  is the Riesz representor of  $a(u, \cdot; \nu)$ , which allows to write the stability constant as

$$\beta(\nu) = \inf_{u \in X} \frac{\|T^\nu u\|_X}{\|u\|_X}. \quad (21)$$

The stability constant can thus be computed by solving the eigenvalue problem  $T^\nu u = \lambda_{\min} u$  for the eigenvalue of minimum magnitude  $\lambda_{\min}$ . Introduce the discrete inner product  $(u, v)_X = u^T \mathcal{X} v$  with elements  $\mathcal{X}_{ij} = (\phi_i, \phi_j)_X$ . Generally, the matrix representing the operator  $T^\nu$  is dense, as  $T^\nu = \mathcal{X}^{-1} A^\nu$ , so that we instead solve the equivalent generalized eigenvalue problem

$$A^\nu u = \lambda_{\min} \mathcal{X} u. \quad (22)$$

With the linear operators  $T^q : X \rightarrow X$  defined by

$$(T^q u, \cdot) = a^q(u, \cdot; \nu), \quad \forall q = 1, \dots, Q_a, \quad (23)$$

the supremizing operator satisfies the same affine expansion as the bilinear form (14)

$$T^\nu u = \sum_{q=1}^{Q_a} \Theta_a^q(\nu) T^q u. \quad (24)$$

### III. REDUCED BASIS MODEL REDUCTION

In the RBM, the reduced order space  $X_N$  onto which the system is projected, is composed of ‘‘snapshot’’ solutions, i.e. field solution vectors  $u(\nu_i)$  at particular parameter locations  $S_N = \{\nu_1, \dots, \nu_N\}$ . To get good approximation properties, while keeping the size  $N$  of the reduced space low, it is essential to choose the snapshot locations  $S_N$  carefully.

This can be achieved in a greedy process [12], which iteratively chooses snapshot locations based on evaluating an error estimator  $\Delta_N(\nu)$  and choosing in each iteration only the snapshot location, which is currently least well approximated. Let  $\Xi$  denote a sufficiently fine, discrete sample of the parameter domain  $D$  and  $\epsilon$  be a prespecified approximation tolerance.

**Algorithm 1:** Greedy Sampling Strategy:

- 1: Choose  $\nu_1 \in \Xi$  arbitrarily
- 2: Solve (12) for  $u(\nu_1)$
- 3: Set  $S_1 = \{\nu_1\}$
- 4: Set  $X_1 = [u(\nu_1)]$
- 5: Set  $N = 1$
- 6: **while**  $\max_{\nu \in \Xi} \Delta_N(\nu) \geq \epsilon$  **do**
- 7:   Set  $\nu_{N+1} = \arg \max_{\nu \in \Xi} \Delta_N(\nu)$
- 8:   Solve (12) for  $u(\nu_{N+1})$
- 9:   Set  $S_{N+1} = S_N \cup \nu_{N+1}$

- 10: Set  $X_{N+1} = [X_N \ u(\nu_{N+1})]$   
 11: Orthonormalize the columns of  $X_{N+1}$   
 12: Set  $N = N + 1$   
 13: **end while**

Let  $u_N$  denote the reduced order field solution, obtained after projecting the weak form onto  $X_N$

$$a(u_N(\nu), v_N; \nu) = f(v_N; \nu), \quad \forall v_N \in X_N. \quad (25)$$

Introducing the error  $e(\nu)$  and the residual  $r(\cdot; \nu)$  as

$$\begin{aligned} e(\nu) &= u(\nu) - u_N(\nu), \\ r(\cdot; \nu) &= f(\cdot; \nu) - a(u_N(\nu), \cdot; \nu), \end{aligned}$$

it holds

$$a(e(\nu), \cdot; \nu) = r(\cdot; \nu).$$

Let  $\hat{e}(\nu)$  denote the Riesz representer of the residual

$$(\hat{e}(\nu), \cdot)_X = r(\cdot; \nu),$$

then it follows

$$a(e(\nu), \cdot; \nu) = (\hat{e}(\nu), \cdot)_X, \quad (26)$$

$$\|r(\cdot; \nu)\|_{X'} = \|\hat{e}(\nu)\|_X. \quad (27)$$

To avoid numerical instabilities, we compute a set of orthonormal basis functions  $\zeta_i$ , such that the reduced order solution has a representation of the form

$$u_N(\nu) = \sum_{n=1}^N \alpha_n(\nu) \zeta_n, \quad (28)$$

for some coefficients  $\alpha_n$ .

#### A. Offline-Online decomposition

The RBM consists of two computational phases. A time-consuming offline phase, in which the greedy sampling is performed and an online phase, where evaluations of the reduced model are performed. Both phases can be clearly separated, as the offline phase passes only prespecified data about the snapshots and error estimation to the online phase. To enable fast evaluations of the reduced order solution and the error estimators, an  $\mathcal{N}$ -independent online phase is required.

Solving system (25) amounts to solving the linear system

$$\sum_{n=1}^N a(\zeta_n, \zeta_m; \nu) \alpha_n(\nu) = f(\zeta_m), \quad 1 \leq m \leq N, \quad (29)$$

where the matrix can be expanded by (14) into

$$\sum_{n=1}^N \left( \sum_{q=1}^{Q_a} \Theta^q(\nu) a^q(\zeta_n, \zeta_m) \right). \quad (30)$$

As the terms  $a^q(\zeta_n, \zeta_m)$  are parameter-independent, they can be precomputed during the offline phase and only small  $N \times N$  matrices need to be stored. During the online phase, the reduced system matrix is formed according to (30) for each parameter configuration and only an  $N \times N$  linear system needs to be solved.

### B. Error Estimation

A rigorous error estimator  $\Delta_N(\nu)$  for the reduced basis approximation is given by

$$\Delta_N(\nu) = \frac{\|r(\cdot; \nu)\|_{X'}}{\beta(\nu)}, \quad (31)$$

which satisfies

$$\|u(\nu) - u_N(\nu)\|_X \leq \Delta_N(\nu), \quad (32)$$

which follows from (19) and (26), or see ([19], [20]).

Often, one is interested in an output quantity of interest, which can be expressed as a linear functional of the field solution  $\ell(u(\nu))$ , and thus in the error

$$|\ell(u(\nu)) - \ell(u_N(\nu))| = |\ell(u(\nu) - u_N(\nu))|.$$

A trivial bound is given by

$$|\ell(u(\nu) - u_N(\nu))| \leq \|\ell(\cdot)\|_{X'} \|u(\nu) - u_N(\nu)\|_X,$$

which usually will not be very sharp. Good a posteriori error bounds on the output quantity can be derived by considering a primal-dual setup, see the section on noncompliant problems in [12].

The computation of  $\beta(\nu)$  for (31) requires the solution of a large scale eigenvalue problem, which is not feasible in an offline-online context. Therefore, the SCM is employed to derive a lower bound  $\beta_{LB}(\nu)$  to the stability constant, which can be used in an offline-online decomposition.

The error estimator  $\Delta_N(\nu)$  is used in the offline phase, to select snapshots within the greedy algorithm, as well as in the online phase to measure the accuracy of the approximation. To ensure online efficiency,  $\mathcal{N}$ -independent computations of the dual norm of the residual as well as  $\beta_{LB}(\nu)$  are required.

1) *Dual norm of the residual:* To compute the dual norm of the residual efficiently, we use the affine expansion [12]

$$\begin{aligned} r(v; \nu) &= f(v) - a(u_N(\nu), v; \nu) \\ &= f(v) - a\left(\sum_{n=1}^N \alpha_n(\nu) \zeta_n, v; \nu\right) \\ &= f(v) - \sum_{n=1}^N \alpha_n(\nu) a(\zeta_n, v; \nu) \\ &= f(v) - \sum_{n=1}^N \alpha_n(\nu) \sum_{q=1}^{Q_a} \Theta_a^q(\nu) a^q(\zeta_n, v). \end{aligned}$$

It holds

$$\begin{aligned} (\hat{e}(\nu), v)_X &= f(v) - \sum_{q=1}^{Q_a} \sum_{n=1}^N \Theta_a^q(\nu) \alpha_n(\nu) a^q(\zeta_n, v), \\ \hat{e}(\nu) &= C + \sum_{q=1}^{Q_a} \sum_{n=1}^N \Theta_a^q(\nu) \alpha_n(\nu) \mathcal{L}_n^q, \end{aligned}$$

with  $C$  and  $\mathcal{L}_n^q$  solutions to associated symmetric, positive definite systems, sometimes referred to as "FE Poisson" problems in the RB literature

$$\begin{aligned} (C, v)_X &= f(v) \quad \forall v \in X, \\ (\mathcal{L}_n^q, v)_X &= -a^q(\zeta_n, v) \quad \forall v \in X, \end{aligned}$$

such that we derive

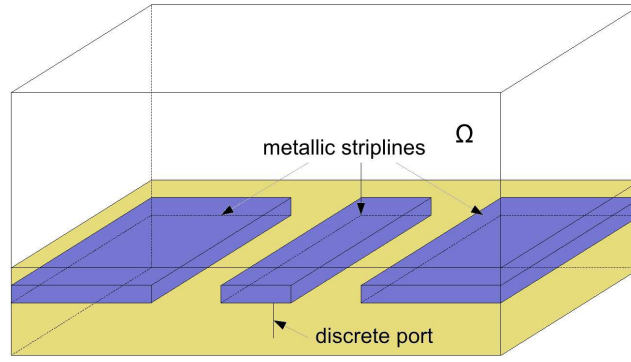


Fig. 1. Coplanar waveguide model.

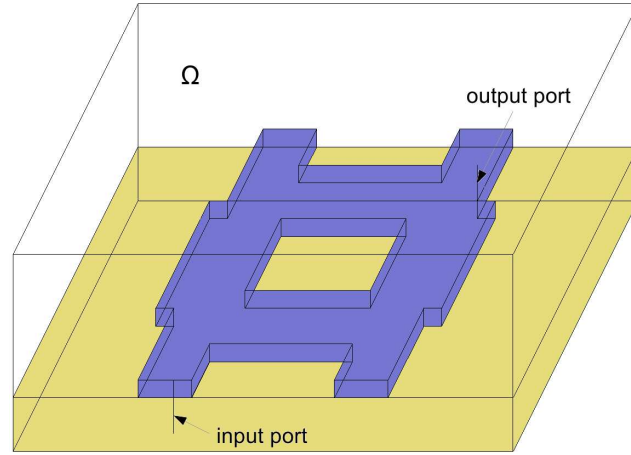


Fig. 2. Branchline coupler model.

$$\begin{aligned}
 \|\hat{e}(\nu)\|_X^2 &= \\
 (C + \sum_{q=1}^{Q_a} \sum_{n=1}^N \Theta_a^q(\nu) \alpha_n(\nu) \mathcal{L}_n^q, \\
 C + \sum_{q=1}^{Q_a} \sum_{n=1}^N \Theta_a^q(\nu) \alpha_n(\nu) \mathcal{L}_n^q)_X \\
 &= (C, C)_X + \sum_{q=1}^{Q_a} \sum_{n=1}^N \Theta_a^q(\nu) \alpha_n(\nu) \times \\
 &\quad \left\{ 2(C, \mathcal{L}_n^q)_X + \sum_{q'=1}^{Q_a} \sum_{n'=1}^N \Theta_a^{q'}(\nu) \alpha_{n'}(\nu) (\mathcal{L}_n^q, \mathcal{L}_{n'}^{q'})_X \right\}.
 \end{aligned}$$

2) *Successive Constraint Method (SCM)*: In Maxwell problems, the SCM has proven to be the computational “bottleneck” of the offline phase ([20]) as it requires to solve a large number of eigenvalue and linear optimization problems. The SCM for the generation of lower bounds to the stability constant is given in Appendix A.

### C. Petrov-Galerkin Reduced Basis

To preserve stability, it is required to achieve that  $\beta_N(\nu) \geq \beta(\nu)$ . This is not automatically satisfied when using standard RB-approximations. Using instead a well-chosen Petrov-Galerkin approximation, the requirement  $\beta_N(\nu) \geq \beta(\nu)$  can be achieved (cf. [19]).

Assume the trial space is spanned by the snapshots  $X_N = \{u(\nu_i) | i = 1, \dots, N\}$  and the test space is chosen using the supremizing operator (20) as  $V_N^\nu = \{T^\nu u(\nu_i) | i = 1, \dots, N\}$ .

The following relation holds between the stability constant of the Petrov-Galerkin reduced model and the full model:

$$\begin{aligned}
\beta_N(\nu) &= \inf_{u \in X_N} \sup_{v \in V_N^\nu} \frac{a(u, v; \nu)}{\|u\|_X \|v\|_X} \\
&= \inf_{u \in X_N} \frac{a(u, T^\nu u; \nu)}{\|u\|_X \|T^\nu u\|_X} \\
&= \inf_{u \in X_N} \frac{\|T^\nu u\|_X}{\|u\|_X} \\
&\geq \inf_{u \in X} \frac{\|T^\nu u\|_X}{\|u\|_X} \\
&= \beta(\nu),
\end{aligned}$$

thus achieving stability preservation.

The parameter-dependent test space  $V_N^\nu$  introduces another affine expansion in the offline-online decomposition, as each trial function  $\zeta_i$  has a corresponding test function  $T^\nu \zeta_i$ , which can be expanded as

$$T^\nu \zeta_i = \sum_{q=1}^{Q_a} \Theta_a^q(\nu) T^q \zeta_i. \quad (33)$$

Using a two-sided approximation, the system (29) becomes

$$\begin{aligned}
\sum_{n=1}^N a(\zeta_n, \sum_{q=1}^{Q_a} \Theta_a^q(\nu) T^q \zeta_m; \nu) \alpha_n(\nu) \\
= \sum_{q=1}^{Q_a} \Theta_a^q(\nu) f(T^q \zeta_m), \quad 1 \leq m \leq N,
\end{aligned} \quad (34)$$

where the left-hand-side can be expanded into

$$\sum_{n=1}^N \left( \sum_{q=1}^{Q_a} \sum_{q'=1}^{Q_a} \Theta_a^q(\nu) \Theta_a^{q'}(\nu) a^q(\zeta_n, T^{q'} \zeta_m) \right) \alpha_n(\nu). \quad (35)$$

During the offline phase, the forms  $a^q(\zeta_n, T^{q'} \zeta_m)$  are generated and stored as small  $N \times N$  matrices and can be efficiently evaluated online.

#### IV. NUMERICAL EXAMPLES

We apply the RBM to two example models<sup>1</sup>, a coplanar waveguide (Fig. 1) and a branchline coupler (Fig. 2). Both models are contained in a shielded box with a PEC ground plate on the bottom. The systems are excited by discrete ports, located between ground plate and metallic components (shown in blue). While the upper part of the models is filled with air, the lower part is filled with a substrate of differing material properties (shown in yellow). For the reference configurations, the parameter-independent matrices of the affine expansion (14) were generated using the finite element package FEniCS [21].

##### A. Coplanar Waveguide

The full model of the coplanar waveguide contains 52,134 degrees of freedom. The discrete port shown in Fig. 1 serves as the input port, the output port is placed at the far side of the waveguide. In the upper part of the model, the relative permittivity is  $\epsilon_r = 1.07$  and the conductivity  $\sigma = 0.01$  S/m. In the lower part, the relative permittivity is  $\epsilon_r = 4.4$  and the conductivity  $\sigma = 0.02$  S/m. The relative permeability is one in the entire domain. The dimensions of the shielded box are 140 mm by 100 mm by 50 mm.

Considered parameters are the frequency in [1.3, 1.6] GHz and the width of the middle stripline within [2.0, 14.0] mm. This is a substantial geometric variation, as the distance between the outer striplines is just 16.0 mm.

To achieve the affine expansion (14), the domain  $\Omega$  is decomposed into subdomains as shown in Fig. 3. On  $\Omega^1$ , the affine transformation  $T^1$  is the identity, while the transformations for the other subdomains can be given in terms of the geometric parameter  $\nu$ . Applying (16) and taking into account the frequency as a second parameter leads to an affine form with  $Q_a = 15$  terms.

<sup>1</sup>The models have been developed within the "MoreSim4Nano" project, "Model Reduction for Fast Simulation of New Semiconductor Structures for Nanotechnology and Microsystems Technology" ([www.moresim4nano.org](http://www.moresim4nano.org)).

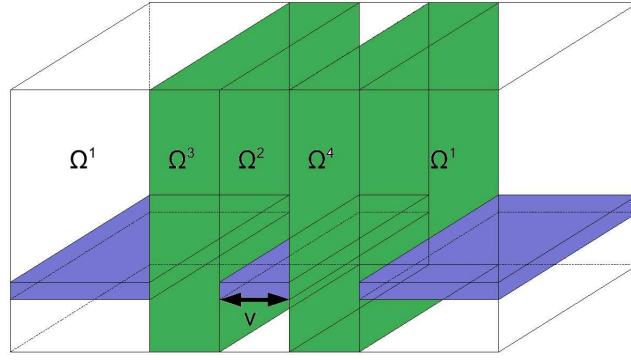


Fig. 3. Coplanar waveguide: selected subdomains.

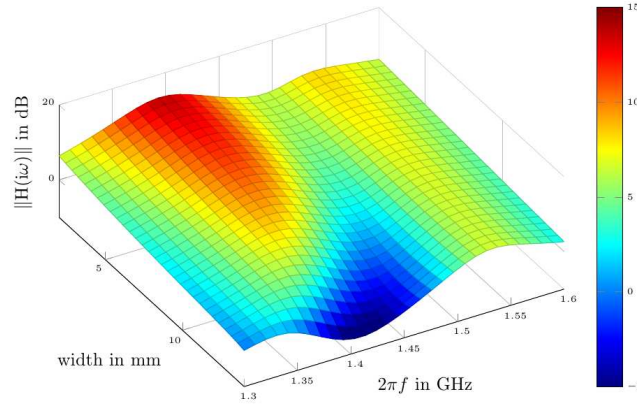


Fig. 4. Coplanar waveguide: transfer function of full order model.

The transfer function plotted over the parametric domain for the full order and reduced order models of dimension  $N = 45$  are shown in Fig. 4 and Fig. 5.

The relative error  $\frac{\|u(\nu) - u_N(\nu)\|_X}{\|u(\nu)\|_X}$  and the error estimator for the relative error  $\frac{\Delta_N}{\|u_N(\nu)\|_X}$  are plotted in Fig. 6 over the reduced basis dimension  $N$ . The maximum and the arithmetic mean are computed over all  $\nu \in \Xi$  for each RB-dimension  $N$ . An exponential convergence of the reduced basis solutions to the full order solutions can be observed.

Due to the large number of affine terms ( $Q_a = 15$ ), an approximation to the lower bound of the stability constant is used. In particular, only the upper bounds are computed (cf. Appendix A), by using a coarse uniform  $10 \times 30$  grid, and the resulting upper bounds are scaled by a factor of 0.5 to achieve lower bounds. Numerical tests showed that the SCM generates sharp upper bounds ([20]), so that this approach is justified.

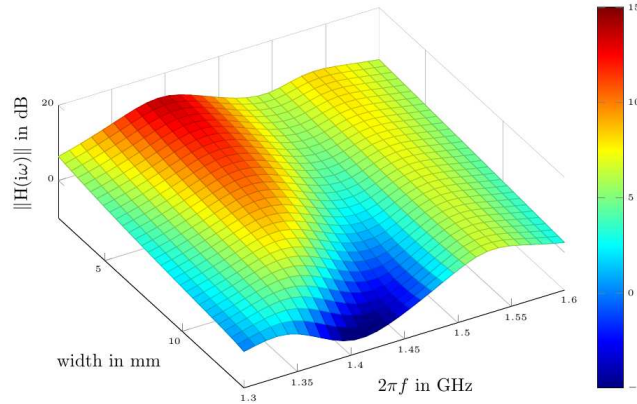


Fig. 5. Coplanar waveguide: transfer function of reduced order model for  $N = 45$ .

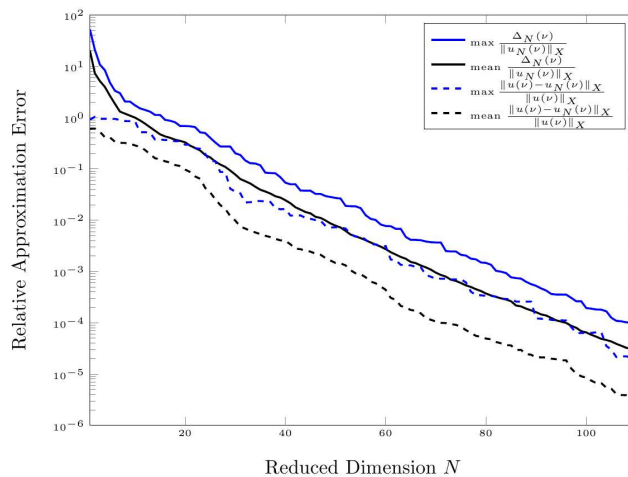


Fig. 6. Relative error in the field solution plotted over the reduced basis dimension  $N$  for the coplanar waveguide.

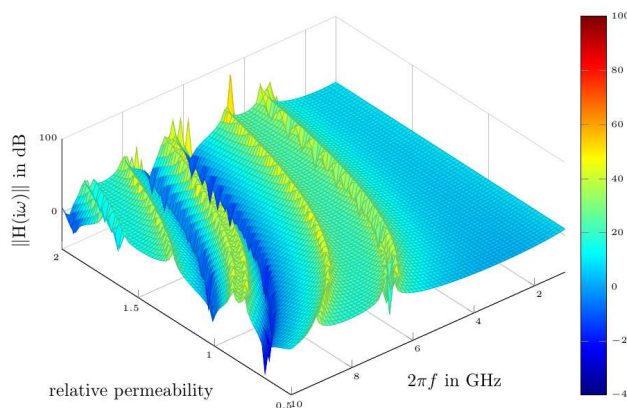


Fig. 7. Branchline coupler: transfer function of full order model.

### B. Branchline Coupler

The full model of the branchline coupler (Fig. 2) contains 27,679 degrees of freedom. In the upper part of the model, the relative permittivity is  $\epsilon_r = 1$  while in the lower part, the relative permittivity is  $\epsilon_r = 2.2$ . The conductivity is zero in the entire domain. The dimensions of the shielded box are 23.6 mm by 22 mm by 7 mm.

Considered parameters are the frequency in  $[1.0, 10.0]$  GHz and the relative permeability which varies within  $[0.5, 2.0]$ .

The transfer function plotted over the parametric domain for the full order and reduced order models of dimension  $N = 25$  are shown in Fig. 7 and Fig. 8.

The relative error  $\frac{\|u(\nu) - u_N(\nu)\|_X}{\|u(\nu)\|_X}$  and the error estimator for the relative error  $\frac{\Delta_N}{\|u_N(\nu)\|_X}$  are plotted in Fig. 9 over the reduced basis dimension  $N$ . The maximum and the arithmetic mean are computed over all  $\nu \in \Xi$  for each RB-dimension  $N$ .

As the branchline coupler model includes several resonances, the error estimator  $\Delta_N$  might strongly overestimate the absolute error  $\|u(\nu) - u_N(\nu)\|_X$  at parameter locations close to resonances. It can thus happen that the greedy algorithm chooses a snapshot location twice, which leads to a "breakdown" of the offline phase. This can be overcome by either using an estimator for the relative error  $\frac{\Delta_N(\nu)}{\|u_N(\nu)\|_X}$  in the greedy sampling (Algorithm 1) or by performing the maximization over  $\Xi \setminus S_N$ .

Due to the difficulty of properly resolving the resonances, the chosen snapshot locations follow the resonance configurations (Fig. 10), as in [20].

### C. Summary of Numerical Results

The computational results are summarized in Table 1. Using the error estimator, a relative error of less than 1% can be guaranteed at a reduced order of  $N = 59$  for the coplanar waveguide, while actually this error is satisfied at an even lower order  $N = 47$ . Similar findings hold for an error tolerance of 0.1%. For the branchline coupler, these error criteria are satisfied at a reduced order of  $N = 21$ . The error estimators show a median effectivity of 10 and 7 respectively, i.e. in the median the estimators will overestimate the actual error by these factors. At resonance configurations and at snapshot locations, the error estimator often strongly overestimates the actual error, so that there is a significant difference between the median and arithmetic mean effectivity.

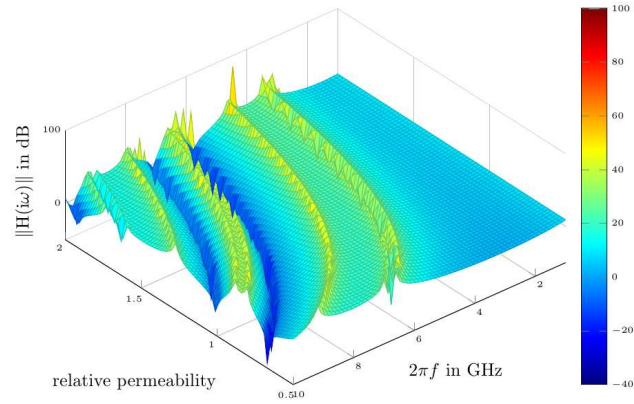


Fig. 8. Branchline coupler: transfer function of reduced order model for  $N = 25$ .

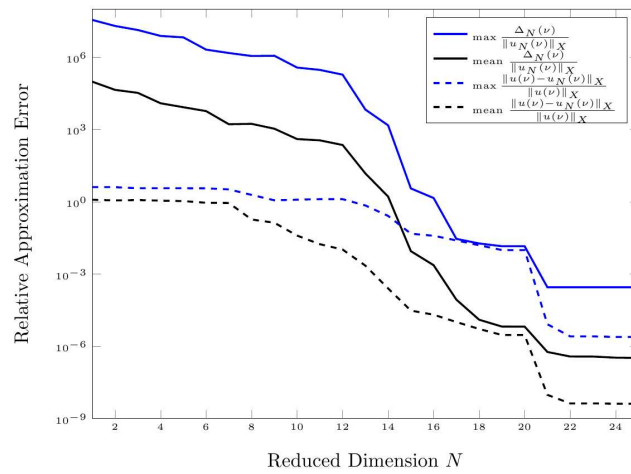


Fig. 9. Relative error in the field solution plotted over the reduced basis dimension  $N$  for the branchline coupler.

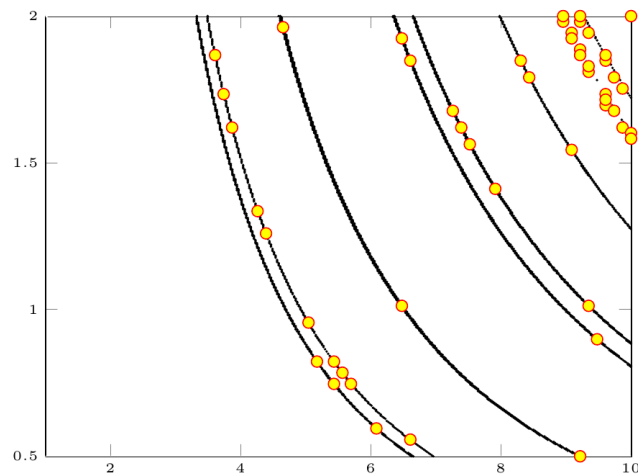


Fig. 10. Chosen snapshot locations (yellow/red) follow the resonance configurations (black). Shown for  $N = 50$ .

TABLE I  
SUMMARY OF RBM PERFORMANCE

	waveguide	coupler
<b>Full Model Order</b>	52,134	27,679
$\min\{N   \max \frac{\Delta_N(\nu)}{\ u_N(\nu)\ _X} \leq 1\%\}$	59	21
$\min\{N   \max \frac{\Delta_N(\nu)}{\ u_N(\nu)\ _X} \leq 0.1\%\}$	83	21
$\min\{N   \max \frac{\ u(\nu) - u_N(\nu)\ _X}{\ u(\nu)\ _X} \leq 1\%\}$	47	21
$\min\{N   \max \frac{\ u(\nu) - u_N(\nu)\ _X}{\ u(\nu)\ _X} \leq 0.1\%\}$	68	21
<b>timing full simulation (all <math>\nu \in \Xi</math>)</b>	7,930s	8,644s
<b>timing reduced simulation (all <math>\nu \in \Xi</math>)</b>	10s ( $N=85$ )	1s ( $N=25$ )
<b>mean effectivity</b>	11	1537
<b>median effectivity</b>	7	10

## V. CONCLUSION

We here presented the certified reduced basis model reduction approach and its application to electromagnetic problems. The RBM reduces models with parametric variations in frequency and geometry as well as material by a factor of about 100. The employed error estimators gave reliable and efficient bounds to the error for each input-output solve of the reduced model. Further research directions are sampling techniques for higher dimensional parameter spaces which leads to interpolation techniques ([22]) and using the RBM in uncertainty quantification (UQ).

## APPENDIX A SUCCESSIVE CONSTRAINT METHOD

The SCM method outlined here, based on [18] and [20], has a quadratic complexity in the number of terms in the affine expansion  $Q_a$ , which can lead to long computation times of the offline phase. An advanced SCM, called natural norm SCM, with linear complexity in  $Q_a$  is presented in [23], which also achieves lower bounds to the stability constant, but is however algorithmically much more involved.

Using (21), the squared inf-sup constant satisfies

$$(\beta(\nu))^2 = \min_{u \in X} \frac{(T^\nu u, T^\nu u)_X}{\|u\|_X^2},$$

which can be expanded as

$$(\beta(\nu))^2 = \min_{u \in X} \sum_{q'=1}^{Q_a} \sum_{q''=q'}^{Q_a} (2 - \delta_{q',q''}) \Theta^{q'}(\nu) \Theta^{q''}(\nu) \frac{(T^{q'} u, T^{q''} u)_X}{\|u\|_X^2}.$$

Symmetrizing the problem using elementary properties of the scalar product (cf. [20]) and defining  $Z_{q'}^{q''}(\nu)$  as  $Z_{q'}^{q''}(\nu) = \Theta^{q'}(\nu) \Theta^{q''}(\nu)$ , it follows

$$(\beta(\nu))^2 = \min_{u \in X} \sum_{q=1}^{Q_a} \left( Z_q^q(\nu) - \sum_{q'=1, q' \neq q}^{Q_a} Z_q^{q'}(\nu) \right) \frac{(T^q u, T^q u)_X}{\|u\|_X^2} + \sum_{q'=1}^{Q_a} \sum_{q''=q'+1}^{Q_a} Z_{q'}^{q''}(\nu) \frac{(T^{q'} u + T^{q''} u, T^{q'} u + T^{q''} u)_X}{\|u\|_X^2}. \quad (36)$$

Introducing the notation  $y_{q',q''}$  for the  $\nu$ -independent parts of (36),

$$\begin{aligned}
y_{q,q}(u) &= \frac{(T^q u, T^q u)_X}{\|u\|_X^2}, \\
y_{q',q''}(u) &= \frac{(T^{q'} u + T^{q''} u, T^{q'} u + T^{q''} u)_X}{\|u\|_X^2}, \quad q'' > q',
\end{aligned}$$

and defining the set  $\mathcal{Y}$  as

$$\mathcal{Y} = \left\{ y = (y_{1,1}, \dots, y_{Q_a, Q_a}) \in \mathbb{R}^{\frac{Q_a(Q_a+1)}{2}} \mid \exists u \in X \text{ s.t. } y_{q,q} = y_{q,q}(u), y_{q',q''} = y_{q',q''}(u) \right\},$$

allows to formulate the stability constant as a minimization problem over  $\mathcal{Y}$

$$(\beta(\nu))^2 = \min_{y \in \mathcal{Y}} \mathcal{J}(\nu; y), \quad (37)$$

with the objective function

$$\mathcal{J} : \mathcal{D} \times \mathbb{R}^{\frac{Q_a(Q_a+1)}{2}} \rightarrow \mathbb{R} \quad (38)$$

$$\begin{aligned}
\mathcal{J}(\nu; y) &= \sum_{q=1}^{Q_a} \left( Z_q^q(\nu) - \sum_{q'=1, q' \neq q}^{Q_a} Z_{q'}^{q'}(\nu) \right) y_{q,q} \\
&\quad + \sum_{q'=1}^{Q_a} \sum_{q''=q'+1}^{Q_a} Z_{q'}^{q''}(\nu) y_{q',q''}.
\end{aligned}$$

The central idea of the SCM is to define sets  $\mathcal{Y}_{LB}$  and  $\mathcal{Y}_{UB}$  such that  $\mathcal{Y}_{UB} \subset \mathcal{Y} \subset \mathcal{Y}_{LB}$  holds, which implies

$$\min_{y \in \mathcal{Y}_{LB}} \mathcal{J}(\nu, y) \leq \min_{y \in \mathcal{Y}} \mathcal{J}(\nu, y) \leq \min_{y \in \mathcal{Y}_{UB}} \mathcal{J}(\nu, y),$$

such that bounds on the discrete inf-sup constant are given by

$$\begin{aligned}
(\beta_{LB}(\nu))^2 &= \min_{y \in \mathcal{Y}_{LB}} \mathcal{J}(\nu, y), \\
(\beta_{UB}(\nu))^2 &= \min_{y \in \mathcal{Y}_{UB}} \mathcal{J}(\nu, y).
\end{aligned}$$

Define the continuity constraint Box  $\mathcal{B}$  and the constraint sample  $C_K$  as

$$\begin{aligned}
\mathcal{B} &= \prod_{q'=1}^{Q_a} \prod_{q''=q'}^{Q_a} \left[ \min_{w \in X} y_{q',q''}(w), \max_{w \in X} y_{q',q''}(w) \right], \\
C_K &= \{\nu_1, \dots, \nu_K\} \subset \Xi.
\end{aligned}$$

The lower bound and upper bound sets are defined as

$$\begin{aligned}
Y_{LB}(\nu, C_K) &= \{y \in \mathcal{B} \mid \mathcal{J}(\nu', y) \geq \beta(\nu'), \forall \nu' \in C_K, \\
&\quad \mathcal{J}(\nu', y) \geq \beta_{LB}(\nu'; C_{K-1}), \forall \nu' \in \Xi \setminus C_K\},
\end{aligned}$$

$$Y_{UB}(C_K) = \{y^*(\nu_k) \mid y^*(\nu_k) = \arg \min_{y \in \mathcal{Y}} \mathcal{J}(\nu_k; y), \nu_k \in C_K\}.$$

This leads to a Linear Program with  $\frac{Q_a(Q_a+1)}{2}$  design variables and  $Q_a(Q_a+1) + |\Xi|$  inequality constraints.

Algorithm 2 summarizes the SCM in pseudocode. The approximation quality can be controlled by the relative error tolerance  $\epsilon_{SCM}$ . Comparing to Algorithm 1 shows that the SCM is also a greedy procedure.

**Algorithm 2: Successive Constraint Method:**

- 1: set  $K = 1$
- 2: choose  $C_K = \{\nu_1\}$  arbitrarily
- 3: compute  $\beta(\nu_1)$
- 4: **while**  $\max_{\nu \in \Xi} \frac{\beta_{UB}(\nu; C_K) - \beta_{LB}(\nu; C_K)}{\beta_{UB}(\nu; C_K)} \geq \epsilon_{SCM}$  **do**
- 5:   set  $\nu_{K+1} = \arg \max_{\nu \in \Xi} \frac{\beta_{UB}(\nu; C_K) - \beta_{LB}(\nu; C_K)}{\beta_{UB}(\nu; C_K)}$
- 6:   compute  $\beta(\nu_{K+1})$
- 7:   set  $C_{K+1} = C_K \cup \{\nu_{K+1}\}$
- 8:   set  $K = K + 1$
- 9: **end while**

## ACKNOWLEDGMENT

The authors would like to thank A. Geranmayeh (former TU Darmstadt) for providing the model descriptions, D.J. Knezevic (Harvard University), K. Veroy-Grepl (RWTH Aachen) and M. Stoll (MPI Magdeburg) for fruitful discussions and helpful advice.

## REFERENCES

- [1] T. Wittig, R. Schuhmann, and T. Weiland, "Model order reduction for large systems in computational electromagnetics," *Linear Algebra and its Applications*, vol. 415, pp. 499 – 530, 2006.
- [2] K. K. Stavrakakis, "Model order reduction methods for parametrized systems in electromagnetic field simulations," Ph.D. dissertation, Technical University Darmstadt, 2012.
- [3] D. Bonin and D. A. Mellichamp, "A unified derivation and critical review of modal approaches to model reduction," *Int. J. Control*, vol. 35, pp. 829 – 848, 1982.
- [4] L. T. Pillage and R. A. Rohrer, "Asymptotic waveform evaluation for timing analysis," *IEEE Trans. Computer Aided Design*, vol. 9, pp. 352 – 366, 1990.
- [5] S. V. Polstyanko, R. Dyczij-Edlinger, and J.-F. Lee, "Fast frequency sweep technique for the efficient analysis of dielectric waveguides," *IEEE Trans. on Microwave Theory and Techniques*, vol. 45, pp. 1118 – 1126, 1997.
- [6] T. Zhou, S. L. Dvorak, and J. L. Prince, "Application of the Pade via Lanczos (PVL) algorithm to electromagnetic systems with expansion at infinity," in *Proc. of 2000 Electronic Components and Technology Conference*, 2000, pp. 1515 – 1520.
- [7] I. Munteanu, T. Wittig, T. Weiland, and D. Ioan, "FIT/PVL circuit-parameter extraction for general electromagnetic devices," *IEEE Transactions on Magnetics*, vol. 36 (4), pp. 1421 – 1425, 2000.
- [8] R. W. Freund, "SPRIM: Structure-preserving reduced-order interconnect macromodeling," in *Proceedings of the 2004 IEEE/ACM International conference on Computer-aided design*, ser. ICCAD '04. IEEE Computer Society, 2004, pp. 80 – 87.
- [9] T. V. Narayanan and M. Swaminathan, "Preconditioned second-order multi-point passive model reduction for electromagnetic simulations," *IEEE Trans. on Microwave Theory and Techniques*, vol. 58, pp. 2856 – 2866, 2010.
- [10] T. Wittig, I. Munteanu, R. Schuhmann, and T. Weiland, "Two-Step Lanczos algorithm for model order reduction," *IEEE Transactions on Magnetics* 38, vol. 2, pp. 673 – 676, 2002.
- [11] A. Bostani and J. P. Webb, "Finite-element eigenvalue analysis of propagating and evanescent modes in 3-d periodic structures using model-order reduction," *IEEE Trans. on Microwave Theory and Techniques*, vol. 60, pp. 2677 – 2683, 2012.
- [12] G. Rozza, D. B. P. Huynh, and A. T. Patera, "Reduced basis approximation and a posteriori error estimation for finely parametrized elliptic coercive partial differential equations," *Arch. Comput. Methods Eng.*, vol. 15, pp. 229 – 275, 2008.
- [13] V. de la Rubia, U. Razafison, and Y. Maday, "Reliable fast frequency sweep for microwave devices via the reduced-basis method," *IEEE Trans. on Microwave Theory and Techniques*, vol. 57, pp. 2923 – 2937, 2009.
- [14] S. Zaglmayr, "High order finite element methods for electromagnetic field computation," Ph.D. dissertation, JKU Linz, 2006.
- [15] P. Monk, *Finite Element Methods for Maxwell's Equations*. The Clarendon Press Oxford University Press, 2003.
- [16] M. A. Grepl, Y. Maday, N. C. Nguyen, and A. T. Patera, "Efficient reduced-basis treatment of nonaffine and nonlinear partial differential equations," *Mathematical Modelling and Numerical Analysis (M2AN)*, vol. 41, pp. 575 – 605, 2007.
- [17] J. Pomplun, "Reduced basis method for electromagnetic scattering problems," Ph.D. dissertation, Free University Berlin, 2010.
- [18] D. B. P. Huynh, G. Rozza, S. Sen, and A. T. Patera, "A successive constraint linear optimization method for lower bounds of parametric coercivity and inf-sup stability constants," *CR Acad. Sci. Paris*, vol. 345, pp. 473 – 478, 2007.
- [19] Y. Maday, A. T. Patera, and D. V. Rovas, "A blackbox reduced-basis output bound method for noncoercive linear problems," *Studies in Mathematics and its Applications*, vol. 31, pp. 533 – 569, 2002.
- [20] Y. Chen, J. S. Hesthaven, Y. Maday, and J. Rodriguez, "Improved successive constraint method based a posteriori error estimate for reduced basis approximation of 2d Maxwell's problem," *ESAIM: M2AN*, vol. 43, pp. 1099 – 1116, 2009.
- [21] A. Logg, K.-A. Mardal, and G. N. Wells, *Automated Solution of Differential Equations by the Finite Element Method*. Springer, 2012.
- [22] F. Ferranti, M. Nakhla, G. Antonini, T. Dhaene, L. Knockaert, and A. E. Ruehli, "Interpolation-based parametrized model order reduction of delayed systems," *IEEE Trans. on Microwave Theory and Techniques*, vol. 60, pp. 431–440, 2012.
- [23] D. B. P. Huynh, D. J. Knezevic, Y. Chen, J. S. Hesthaven, and A. T. Patera, "A natural-norm successive constraint method for inf-sup lower bounds," *Comput. Methods Appl. Mech. Engin.*, vol. 199, pp. 29 – 33, 2010.